Rev.Adv.Mater.Sci. 18(2008) 536-540

INITIAL DYNAMIC SUSCEPTIBILITY OF BIOCOMPATIBLE MAGNETIC FLUIDS

P.C. Morais[1], L.B. Silveira[2], A.C. Oliveira[1] and J.G. Santos[2]

[1]niversidade de Brasília, Instituto de Física, Núcleo de Física Aplicada, Brasília DF 70910-900, Brazil
[2]Fundação Universidade Federal de Rondônia, Departamento de Cięncias Exatas e da Natureza, Porto Velho RO 78961-970, Brazil

Received: March 29, 2008

Abstract. Biocompatible magnetic fluid samples containing magnetite nanoparticle surface-coated with dextran or dimercaptosuccinic acid (DMSA) were investigated using dynamic susceptibility measurements. Room-temperature investigations of the susceptibility peak position (imaginary component) as a function of the samples' nanoparticle concentrations (from 10^{14} to 10^{16} nanoparticle/cm^3) were performed in the limit of low external applied magnetic field (150 Oe). Analyzes of the imaginary components include both the particle size polydispersity profile and particle-particle interaction.

1. INTRODUCTION

The design and synthesis of biocompatible magnetic fluids (BMFs) has attracted intense interest in recent years. Magnetohyperthermia has been pointed out as a very promising approach for cancer therapy [1-3]. However, the efficiency of the magnetohyperthermia of targeted cells for instance depends upon the energy absorption from an external applied AC field (low-amplitude). This study reports on magnetic investigation of dextran-coated and dimercaptosuccinic acid (DMSA)-coated magnetite-based biocompatible magnetic fluids using dynamic susceptibility (DS) measurements. Here, special emphasis is devoted to the investigation of the concentration dependence of the susceptibility peak frequency (imaginary component) in the limit of megahertz and low applied magnetic fields.

2. EXPERIMENTAL RESULTS AND DISCUSSION

The biocompatible magnetic fluid (BMF) samples were prepared according to the standard procedure described in the literature [4]. The stock samples were diluted to produce five diluted samples with particle concentration in the range from 10^{14} to 10^{16} particle/cm^3. The transmission electron microscopy (TEM) micrographs of the surface-coated magnetite nanoparticles samples were recorded using a JEOL-1010 system. Fig. 1 shows the particle size histograms obtained from the TEM data, which were curve-fitted using the log-normal distribution function. The average particle diameter (diameter dispersion) obtained from the TEM data were 3.1 (0.26) nm and 5.6 (0.22) nm for the dextran-coated and DMSA-coated magnetite nanoparticles, respectively.

The room-temperature DS measurements (real and imaginary components), under an applied steady field of 150 Oe (initial susceptibility), were carried out using a home-made Robinson oscillator operating in the MHz region (13-37 MHz). Such experimental setup has been successfully used to investigate magnetic nanoparticles dispersed in polymeric-based composites [5,6]. The description of the imaginary component (χ'') of the low-field DS

Corresponding author: P.C. Morais, e-mail: pcmor@unb.br

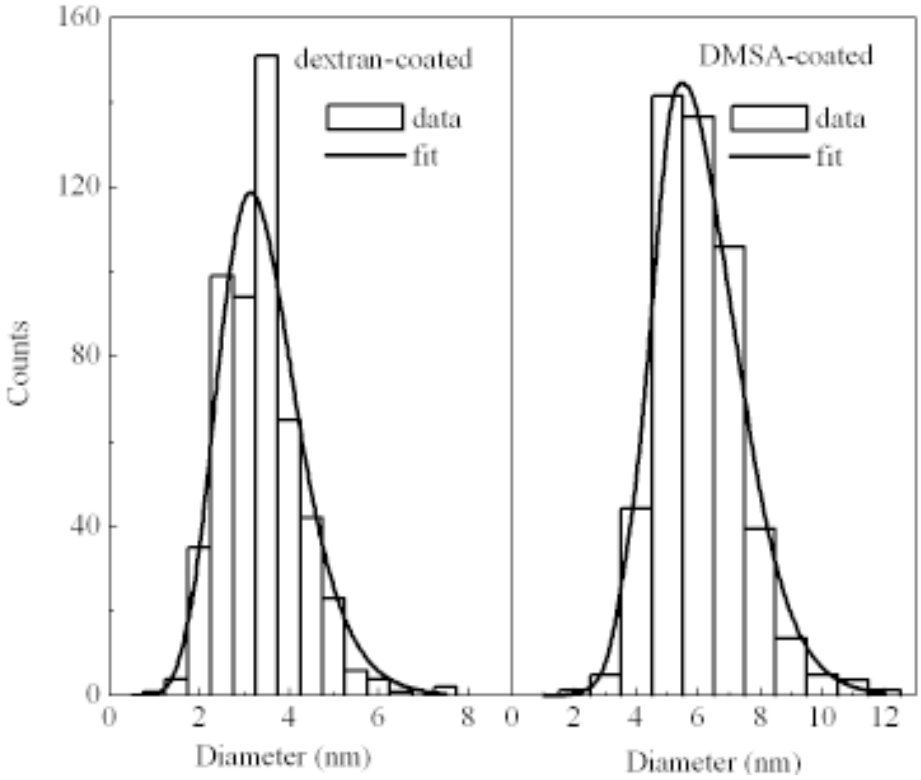

Fig. 1. Particle size histograms of the dextran-coated sample (left panel) and the DMSA-coated sample (right panel). The solid lines represent the best curve fitting using the log-normal distribution function.

curve is based on the model discussed by El-Hilo *et al.* [7]. The model allows one to include the particle-particle interaction via the effect of the particle concentration upon the imaginary susceptibility component. According to El-Hillo *et al.* [7], the initial susceptibility curve description is provided by:

$$\chi'' = A\int_0^{V_b} g(\omega,T)Vf(V)dV + B\int_{V_b}^{\infty} g(\omega,T)f(V)dV + C\int_0^{\infty} g(\omega,T)V^3 f(V)dV, \quad (1)$$

with $g(\omega,T) = \omega\tau_0\exp(\beta KV)/[1+ \omega\tau_0\exp(\beta KV)]$. A, B and C are parameters obtained from the fitting of the frequency-dependence of the low-field DS curves. The first two integrals in Eq. (1) account for non-interacting nanoparticles as follows: the first integral describes the contribution due to the superparamagnetic particles whereas the second integral accounts for the blocked nanoparticles. The third integral of Eq. (1) represents the contribution to the initial susceptibility due to the dipolar interactions. The particle volume polydispersity profile of the samples is accounted by the log-normal distribution function $f(V)$, whereas $g(\omega,T)$ describes the Debye approximation with $\beta = 1/kT$.

The relaxation of the nanoparticle magnetic moment for uniaxial anisotropy is given by [5,8]:

$$f = f_0 \exp(-\Delta E / kT), \quad (2)$$

where $\Delta E = KV + \alpha\mu^2 c$ is the height of the energy barrier. The first term in ΔE describes the effective anisotropy energy, whereas the second term in ΔE describes the dipolar interaction energy. The dipolar coupling constant, nanoparticle magnetic moment, and nanoparticle concentration are described by α, $\mu = M_S V$, and c, respectively.

Fig. 2 shows the DS imaginary component of the dextran-coated magnetite nanoparticles dispersed as a BMF sample. The BMF sample based on DMSA-coated magnetite nanoparticles displays similar DS imaginary components. The nanoparticle concentration of both samples was

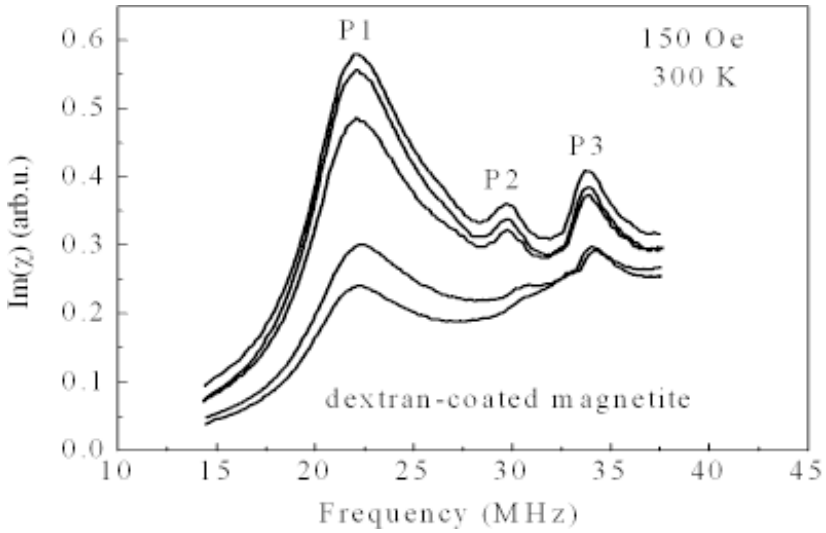

Fig. 2. Imaginary components of the dynamical susceptibility at room-temperature and under 150 Oe steady field. Curves from top to bottom correspond to magnetic fluid samples based on dextran-coated magnetite nanoparticles containing $4.9 \cdot 10^{16}$; $2.4 \cdot 10^{16}$; $9.6 \cdot 10^{15}$, $4.9 \cdot 10^{15}$, and $4.9 \cdot 10^{14}$ nanoparticle/cm^3.

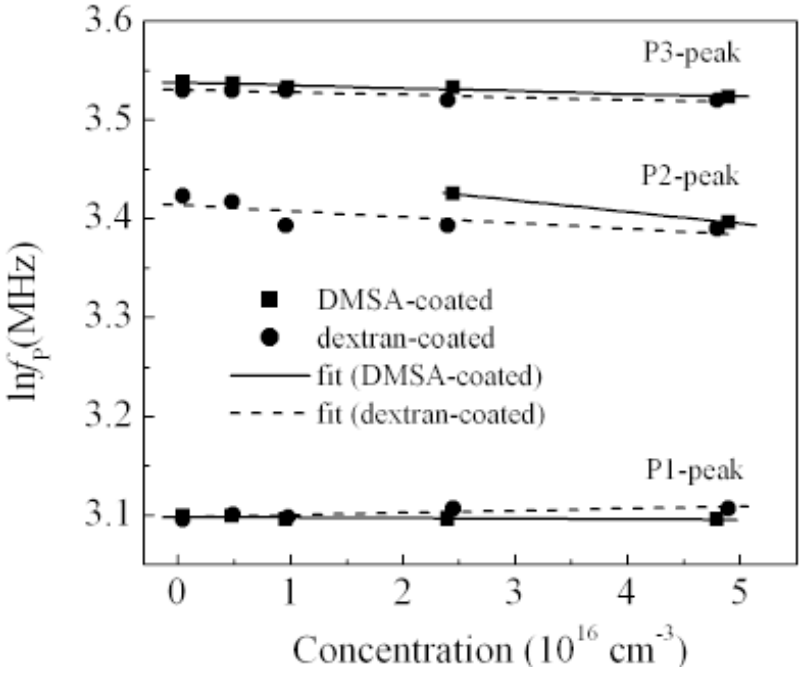

Fig. 3. Peak frequency versus nanoparticle concentration. Symbols represent the best fitted values of the peak positions P1, P2, and P3 for the DMSA-coated (■) and dextran-coated (●) samples. Solid (DMSA-coated) and dashed (dextran-coated) lines represent the best fitting of the data using Eq. (2).

varied in the range from 10^{14} to 10^{16} cm^{-3}. Note from Fig. 2 the presence of three well-defined DS peaks around 22 MHz, 30 MHz, and 34 MHz named P1, P2, and P3, respectively. Recent zero-field measurements revealed that all the DS peaks show a monotonic shift to higher frequencies upon dilution of the BMF sample [9]. However, for the dextran-coated BMF sample under non-zero external field (150 Oe) P1-peak shows the reverse behaviour, namely the susceptibility peak position shifts to lower frequencies upon dilution of the BMF sample.

Symbols in Fig. 3 represent the DS peak positions P1, P2, and P3 as a function of the

nanoparticle concentration. Solid lines in Fig. 3 represent the best fit of the data according to Eq. (2). Except for the P1-peak (see Fig. 3) the data related to the dextran-coated (●) nanoparticles are always running below the data related to the DMSA-coated (■) nanoparticles. According to Eq. (2) this finding indicates a difference in the effective anisotropy energy (*KV*) between the two samples. As the average particle diameter of magnetite surface-coated with dextran (3.1 nm) is smaller than the average particle diameter of the DMSA-coated magnetite (5.6 nm) the effective anisotropy constants of the two samples are quite different. From previous investigation of the same samples (zero field data) we found the values of $4.6 \cdot 10^5$ J/m^3 and $7.8 \cdot 10^4$ J/m^3 for the effective anisotropy constant of the dextran-coated and DMSA-coated magnetite nanoparticles [9]. Note that the anisotropy constant of bulk magnetite is about $1.9 \cdot 10^4$ J/m^3 [10]. We argue that the difference in effective anisotropy values we found for the surface-coated nanoparticles could be due to both the difference in the surface-coating species and different contributions due to surface anisotropy, via differences in particle diameter and the dependence of the surface anisotropy on the nanoparticle size.

Analysis of the P1-peak however leads to new insights regarding the experiments performed under non-zero and zero external fields. We first notice that the multi-peak structure shown in Fig. 2 has been assigned to different magnetic structures within the magnetic fluid sample. At room temperature and under zero external fields we claim that most of the magnetic units in suspension are composed of isolated nanoparticles. However, application of external fields, even weak fields, induces particle-particle coupling in nanoparticle-based arrays. Further, two types of dimer structures can be identified, namely, coherent and fanning modes, being the fanning configuration more likely (lower free energy) than the coherent one. It is well know that the magnetic permeability of the fanning configuration peaks at higher fields than the coherent configuration. In other words, the two structures observed at the higher frequency ends in Fig. 2 should be associated with dimers. Based on this model picture the unusual behaviour observed for P1-peak associated to the dextran-coated magnetite-based BMF sample, in regard to the concentration dependence of the peak frequency at non-zero field, could be understood as follows. Under 150 Oe isolated nanoparticles within the BMF sample tend to stick together building dimers. As the nominal nanoparticle concentration increases the dimer population increases, thus reducing the monomer population. Such effect is much more pronounced for the dextran-coated than for the DMSA-coated magnetite. That happens because of both the higher effective magnetocrystalline anisotropy associated to the dextran-coated magnetite ($4.6 \cdot 10^5$ J/m^3) compared to the DMSA-coated magnetite ($7.8 \cdot 10^4$ J/m^3) and the smaller average diameter of the dextran-coated magnetite (3.1 nm) compared to the DMSA-coated magnetite (5.6 nm). While higher effective magnetocrystalline anisotropy values favour dimers formation more effectively, smaller diameter values bring nanoparticles more close together in more stable structures. Finally, taking into account all the points discussed in this paragraph it becomes easy to understand why only two P2-peaks were resolved for the DMSA-coated magnetite, just at the higher concentration end, as plotted in Fig. 3.

Data shown on Fig. 3 (P2 and P3 peaks) allow us to obtain the dimer dipolar constant (*á*) values. In order to exemplify this procedure we shall use the data from the dextran-coated magnetite nanoparticle, for it provides experimental data in the whole range of nanoparticle concentration. From the linear fit shown on Fig. 3 (dashed lines) the slope ($\alpha\mu^2/kT$) values were obtained: $6.06 \cdot 10^{-19}$ and $2.51 \cdot 10^{-19}$ for P2-peak and P3-peak, respectively. Considering the values of the magnetite bulk magnetization (471 Gauss), the room temperature (300K) and the average nanoparticle diameter (3.1 nm) the dipolar constants were calculated. We found $\alpha = 4.66 \cdot 10^3$ erg/(Gauss·cm^3)^2 and $\alpha = 1.93 \cdot 10^3$ erg/(Gauss·cm^3)^2 for P2-peak and P3-peak, respectively. The bulk saturation magnetization was recently used to estimate the coupling of magnetite nanoparticles in a dimer structure [11]. The drawback of the present approach is that it does not provides independent determination of nanoparticle magnetic moment (μ) and dipolar coupling constant (α).

3. CONCLUSION

Dynamic susceptibility measurements were used to investigate magnetite-based biocompatible magnetic fluid samples. Two distinct surface-coating molecular species were used to produce the magnetic fluid samples, namely dextran and dimercaptosuccinic acid. Three well-resolved peaks were identified in the susceptibility imaginary curves. Under applied 150 Oe the peak positions were investigated as a function of the nanoparticle concentration in the range from 10^{14}

to 10^{16} cm^{-3}. The susceptibility imaginary component analyzes took into account the superparamagnetic particles, the blocked particles, particle-particle interactions, and the particle size polydispersity profile. Our investigation shows an unusual behaviour associated to the lower frequency peak of the dextran-coated magnetite nanoparticles, which shifts to lower frequencies as the nominal nanoparticle increases. This finding was interpreted as the signature of the higher tendency the dextran-coated nanoparticles (five fold magnetocrystalline anisotropy value and half average size) have to build dimers as compared to the DMSA-coated nanoparticles. Thus, for the dextran-coated magnetite the increase of the nominal nanoparticle concentration under non-zero external fields results in an effective reduction of the monomer concentration. This tendency recovers the usual behaviour of P1-peak as explained by Eq. (2).

ACKNOWLEDGEMENTS

This work was partially supported by the Brazilian agencies FINATEC and MCT/CNPq.

REFERENCES

[1] C.C. Berry and A.S.G. Curtis // *J. Phys. D: Appl. Phys.* **36** (2003) R198.

[2] P.R. Stauffer // *Int. J. Hyperthermia.* **21** (2005) 731.

[3] M.H.A. Guedes, N. Sadeghiani, D.L.G. Peixoto, J.P. Coelho, L.S. Barbosa, R.B. Azevedo, S. Kückelhaus, M.F. Da Silva, P.C. Morais and Z.G.M. Lacava // *J. Magn. Magn. Mater.* **293** (2005) 283.

[4] P.C. Morais, R.L. Santos, A.C.M. Pimenta, R.B. Azevedo and E.C.D. Lima // *Thin Sol. Films* **515** (2006) 266.

[5] A.F.R. Rodriguez, A.C. Oliveira, P.C. Morais, D. Rabelo and E.C.D. Lima // *J. Appl. Phys.* **93** (2003) 6963.

[6] L.B. Silveira, J.G. Santos, A.C. Oliveira, A.C. Tedesco, J.M. Marchetti, E.C.D. Lima and P.C. Morais // *J. Magn. Magn. Mater.* **272-276** (2004) 1195.

[7] M. El-Hilo, K. O'Grady and R.W. Chantrell // *J. Magn. Magn. Mater.* **114** (1992) 295.

[8] L. Néel // *C.R. Acad. Sci.* **228** (1949) 664.

[9] P.C. Morais, J.G. Santos, L.B. Silveira and A.C. Oliveira // *J. Alloys Compd,* in press.

[10] B. Payet, D. Vincent, L. Delaunay and G. Noyel // *J. Magn. Magn. Mater.* **186** (1998) 168.

[11] A.F. Bakuzis, J.G. Santos, A.R. Pereira and P.C. Morais // *J. Appl. Phys.* **99** (2009) 08C301.